Histol Histopathol (2023) 38: 549-557

http://www.hh.um.es

Histology and Histopathology
From Cell Biology to Tissue Engineering

ORIGINAL ARTICLE **Open Access**

MiR-29c-3p represses gastric cancer development via modulating MEST

Honghai Li[1], Jieqing Lv[1], Jindao Wang[3], Haifeng Wang[1] and Liang Luo[2]

[1]Department of Gastrointestinal Surgery, [2]Department of Radiotherapy and [3]Department of Endoscopy Center, Shaoxing People's Hospital, Shaoxing Hospital of Zhejiang University, Shaoxing City, Zhejiang Province, PR China

Summary. Gastric cancer (GC) triggers a great number of deaths worldwide. Although great efforts have been made in treating this cancer, GC patients' survival rate remains unsatisfactory. An increasing amount of evidence indicates that miR-29c-3p inhibits cancer progression. However, the mechanism of miR-29c-3p in GC remains to be fully defined. Hence, this work aimed to analyze the underlying mechanism of miR-29c-3p in GC. Outcomes showed marked downregulation of miR-29c-3p in GC tissue and cell lines. Functional experiments exhibited that miR-29c-3p repressed GC cell malignant behaviors. Moreover, bioinformatics analysis and dual-luciferase reporter gene detection indicated that MEST was targeted by miR-29c-3p. Rescue assay further proved that MEST participated in functions of miR-29c-3p in GC. To sum up, miR-29c-3p/MEST signaling pathway suppressed formation of malignant phenotypes of GC, and targeting the signaling pathway may be a new method for treating GC.

Key words: Gastric cancer, miR-29c-3p, MEST, Proliferation, Migration, Invasion

Introduction

Gastric cancer (GC), originating from gastric mucosa epithelium in the digestive system, triggers a considerable number of deaths globally due to its high morbidity and a lack of effective treatments (Han et al., 2019). More than 70% of GC and related deaths are from developing countries, wherein approximately 50% cases are Chinese (Liu et al., 2016). Since GC symptoms are unclear in the early stage, over 80% of GC patients are diagnosed in the advanced stage (Ferlay et al., 2010; Zhang et al., 2017a). Recurrence and metastasis of advanced GC due to deficient diagnosis in the early stage are the main reasons for patient deaths.

At present, combined chemotherapy regimens (two or three cell cytotoxic drugs) can be used to treat advanced GC (Ajani et al., 2013). However, chemotherapy causes many adverse effects and reduces human body immunity. With the advent of precision medicine and promotion of targeted drugs, targeted therapy brings good news for GC patients. For instance, HER2-targeted herceptin and vascular endothelial growth factor receptor (VEGFR2)-targeted tyrosine kinase inhibitor (TKI) apatinib can both remarkably improve the survival and prognosis of advanced-stage GC patients (McGuire et al., 2015).

MicroRNAs (miRNAs) can post-transcriptionally regulate gene expression (Raitoharju et al., 2014). Moreover, miRNA suppresses target mRNA translation or accelerates its degradation via modulating gene expression, thereby participating in biological processes, like cell metabolism, differentiation, migration, and apoptosis, and inhibiting or promoting cancer progression (Wu et al., 2019). Recently, a study elaborated that miR-29 family members are relevant to various tumor expressions (Morita et al., 2013). For example, miR-29c-3p overexpression markedly represses cell malignant behaviors and tumor growth in hepatocellular carcinoma (HCC) (Wu et al., 2019). MiR-29c-3p inhibition facilitates ovarian cancer cell epithelial-mesenchymal transition (EMT) (Xu et al., 2020). Nevertheless, the functions of miR-29c-3p in GC have been less studied.

Herein, bioinformatics predicted that miR-29c-3p was notably downregulated in GC tissue samples and cells. We then identified MEST as targeted by miR-29c-3p through bioinformatics analysis and experiments. MEST and miR-29c-3p are considered as important participants in cancers (Zhang et al., 2017b; Ruan and Zhao, 2019), but their cooperation in GC has not been demonstrated. Hence, the mechanism of miR-29c-3p and MEST in GC were deeply explored to provide a novel

Corresponding Author: DR. Liang Luo, Department of Radiotherapy, Shaoxing People's Hospital, Shaoxing Hospital of Zhejiang University, No.568 of Zhongxing North Road, Shaoxing City, Zhejiang Province, 312000, PR China. e-mail: luolianggg@163.com

DOI: 10.14670/HH-18-537

idea for the therapeutic targeting of GC.

Materials and methods

Bioinformatics approaches

Total RNA sequencing data and mature miRNA expression data in The Cancer Genome Atlas-Stomach Adenocarcinoma (TCGA-STAD) were accessed from TCGA (https://portal.gdc.cancer.gov/) database. After screening, miRNA expression data were required, including 444 cancer tissue samples and 45 normal tissue samples, so were mRNA expression data, including 373 cancer tissue samples and 32 normal tissue samples. Differential analysis was carried out on the miRNAs and mRNAs with R package "edgeR" based on the downloaded data. After the target miRNA was determined through researching references, the mRNAs regulated by it were predicted by using mirDIP (http://ophid.utoronto.ca/mirDIP), TargetScan (http://www.targetscan.org/vert_72/), miRWalk (http://mirwalk.umm.uni-heidelberg.de/), miRDB (http://mirdb.org/), and starBase (http://starbase.sysu.edu.cn/) databases. The predicted mRNAs and differential mRNAs were overlapped, and the correlation between the overlapped mRNAs and the target miRNA was calculated.

Cell culture and transfection

Human GC cell lines AGS (BNCC338141), SGC-7901 (BNCC100674), BGC-823 (BNCC100086) and MKN-45 (BNCC337682), and gastric mucosa epithelial cell line GES-1 (BNCC337969) were purchased from BeNa Culture Collection (BNCC). BGC-823, MKN-45, and SGC-7901 were preserved in Roswell Park Memorial Institute (RPMI) -1640 medium with 10% fetal bovine serum (FBS). AGS was preserved in F-12K medium with 10% FBS. GES-1 was preserved in high-glucose Dulbecco's modified Eagle medium (DMEM) added with glutamine and sodium pyruvate containing 10% FBS. The culture was processed with 5% CO_2 at 37°C in an incubator.

MiR-29c-3p mimic, oe-MEST and corresponding negative controls (NCs) synthesized by RiboBio were transiently transfected using Lipofectamine 2000 kit (Invitrogen). The transfection efficiency was analyzed by qRT-PCR.

qRT-PCR

Total RNA isolation was done by taking TRIzol kit (Invitrogen). RNA was identified through agarose gel electrophoresis (AGE). High-Capacity RNA-to-cDNA kit was used for reverse transcription to quantify miRNA. The abundance of miR-29c-3p was measured with Taq Man probe (Roche) and Master Mix (Thermo Fisher Scientific). U6 was the internal control for miR-29c-3p. Equivalent total RNA was reversely transcribed with ReverTra®qPCR RT Master Mix (Toyobo) to quantify mRNA. qRT-PCR assay was conducted on Bio-rad IQ5 software by using TransStart Green qPCR SuperMix (TransGen Biotech). GAPDH was the internal reference for MEST. All primer sequences are shown in Table 1.

Western Blot

Separation of total proteins was in radio immunoprecipitation assay buffer (Beyotime). Equivalent proteins were separated on sodium dodecyl sulfate polyacrylamide gel electrophoresis, followed by transferring onto a polyvinylidene fluoride membrane. Next, the membrane was blocked with 5% skim milk for 60 min at room temperature, and incubated with primary antibodies at 4°C overnight. After 3 washes with phosphate buffered saline with tween 20 (PBST), secondary antibody IgG H&L (ab6721, 1:5000, Abcam,) coupled with horseradish peroxidase was introduced to incubate the membrane. Afterwards, chemiluminescence analysis was undertaken by using enhanced chemiluminescence (ECL) -Plus kit (Amersham Biosciences). Primary antibodies were antibodies against MEST (ab230114, 1:5000, Abcam) and GAPDH (ab9485, 1:2500, Abcam).

Dual-luciferase reporter analysis

Wild type (WT) or mutant (MUT) MEST 3'-UTR sequences were cloned into psi-DHECK vectors (Promega) (Zhou et al., 2018). Lipofectamine 2000 (Invitrogen) was applied to transfect BGC-823 cells. Luciferase activity was evaluated by dual-luciferase reporter gene system (Promega) on a photometer (Berthold Technologies). Firefly luciferase activity was converted in the form of Renilla luciferase activity.

Colony formation detection

Equivalently transfected GC cells were seeded in 6-well plates and cultured at 37°C. 6-9 days later, the medium was discarded, and the plates were washed with phosphate buffer saline (PBS). Thereafter, the system was fixed with methyl alcohol and dyed with crystal violet. Colonies (more than 50 cells) were photographed

Table 1. qRT-PCR primer list.

Target gene	Primer (5'-3')
miR-29c-3p	F: GAAAGCCACCACGATGCAACAGACAAATTCTGA R: TCTGTTGCATCGTGGTGGCTTTCATACTATATC
U6	F: CTCGCTTCGGCAGCACA R: AACGCTTCACGAATTTGCGT
MEST	F: TGTGGGTGTGGTTGGAAGTC R: CCTCAAGGTCAGACCCTTCC
GAPDH	F: GGAGCGAGATCCCTCCAAAAT R: GGCTGTTGTCATACTTCTCATGG

by Nikon camera and counted.

Cell counting kit-8 (CCK-8) assay

GC cells BGC-823 were suspended in RPMI-1640 with 10% FBS and inoculated into 96-well plates (2×10^3 cells/well). 10 uL CCK-8 reagent (Dojindo) was supplemented to each well after 0, 24, 48 and 72h of cell culture. Then, cells were cultured for another 2h. Finally, absorbance was detected at 450 nm.

Transwell assay

Transwell chamber (Corning) containing Matrigel was utilized for cell invasion detection. After 48h of transfection, while 4×10^3 cells in serum-free medium were transferred to the upper chamber, 10% FBS medium was placed into the lower chamber. After 48h, the unmoved cells were wiped, while the invaded ones were fixed in methyl alcohol and dyed with 0.1% crystal violet. An inverted microscope was utilized to count cells.

Wound healing assay

Transfected cells were seeded into 6-well plates (1×10^5 cells/well). When cells reached 80% confluency, cell monolayers were scraped to create a wound. Afterwards, cells were incubated in serum-free medium for 24h and photographed at 0 and 24h. Migrating distance was measured. Each group was settled in 3 parallel wells.

Data analysis

Data are presented as mean ± standard deviation from at least 3 independent assays. SPSS 17.0 software (SPSS Inc.) was applied for statistical analysis. Independent-samples t-test or Student's t-test was introduced to compare two groups. $p<0.05$ denoted a statistically prominent difference.

Results

MiR-29c-3p expresses relatively low in GC cells

According to TCGA-STAD data, miR-29c-3p was prominently downregulated in GC (Fig. 1A). Further verification of the result was carried out based on qRT-PCR. It was discovered that miR-29c-3p level decreased more in GC cells than in normal human gastric mucosa epithelial cells. Furthermore, GC cell BGC-823, in which the lowest miR-29c-3p expression was presented (Fig. 1B) made itself our subject for following analyses.

MiR-29c-3p upregulation can repress GC cell proliferation, migration and invasion

Thereafter, we explored how miR-29c-3p functions in GC cells. Firstly, miR-29c-3p expression in BGC-823 cells transfected with miR-29c-3p mimic or mimic NC was assayed by qRT-PCR. A significant high miRNA level was shown in miR-29c-3p mimic group (Fig. 2A). CCK-8 and colony formation assays suggested that the proliferation of GC cells was prominently down-regulated in miR-29c-3p mimic group (Fig. 2B-C). Besides, wound healing assay verified that GC cell migration in miR-29c-3p mimic group was repressed compared with the control group (Fig. 2D). Transwell invasion assay suggested that GC cell invasive ability in miR-29c-3p mimic group was evidently more strongly

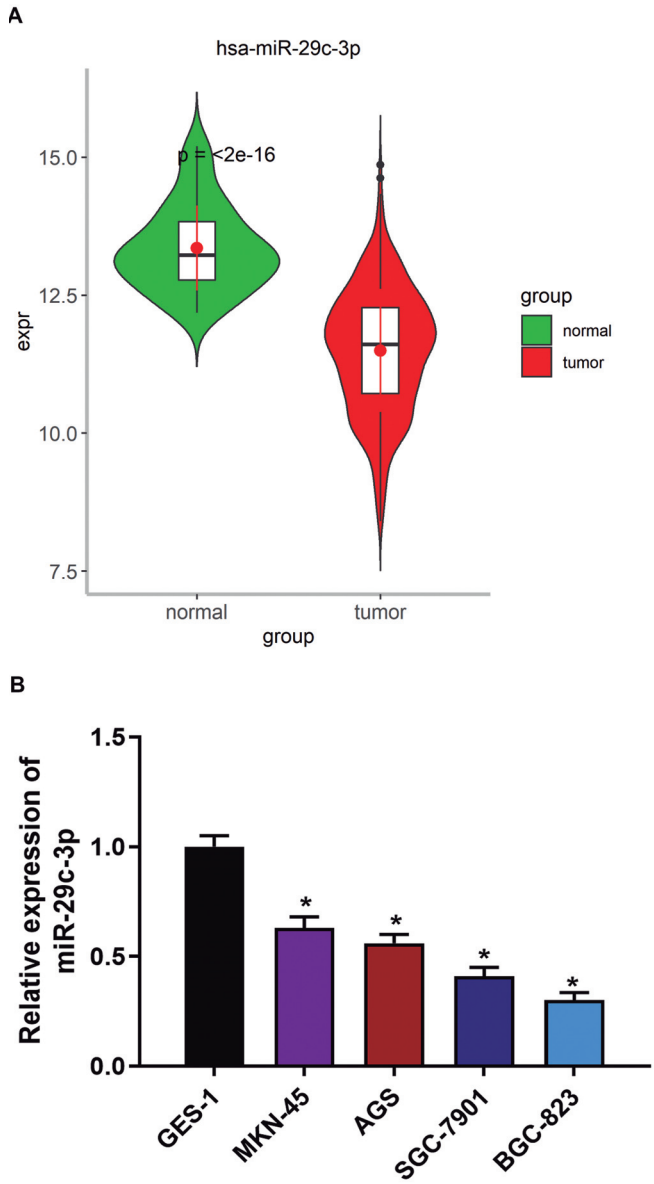

Fig. 1. Low level of miR-29c-3p in GC cells. **A.** TCGA-STAD data presented significant miR-29c-3p downregulation in GC. **B.** MiR-29c-3p expression in normal gastric mucosa epithelial cells and GC cells. (*$p<0.05$)

inhibited than in its negative counterpart (Fig. 2E). The above experimental results were consistent with each other. Hence, we thought that miR-29c-3p upregulation repressed GC cell malignant behaviors.

MEST may be targeted by miR-29c-3p and it is upregulated in GC cells

To further research the downstream mechanism of miR-29c-3p, differential analysis was undertaken on mRNAs in TCGA-STAD. 1,662 differentially expressed mRNAs (DEmRNAs) were acquired (upregulated mRNAs: 775, downregulated mRNAs: 887) (Fig. 3A). Targets of miR-29c-3p were predicted by 5 databases. Afterward, the predicted mRNAs were overlapped with upregulated DEmRNAs and we obtained 4 mRNAs (Fig. 3B). Among them, the strongest negative correlation was found between MEST and miR-29c-3p (Fig. 3C), therefore MEST was predicted to be a target of miR-29c-3p. MEST expression in TCGA was analyzed, and it was discovered that MEST was prominently upregulated in GC tissue samples (Fig. 3D). As illustrated by qRT-PCR and western blot, MEST mRNA and protein expression levels were higher in GC cells than in normal gastric

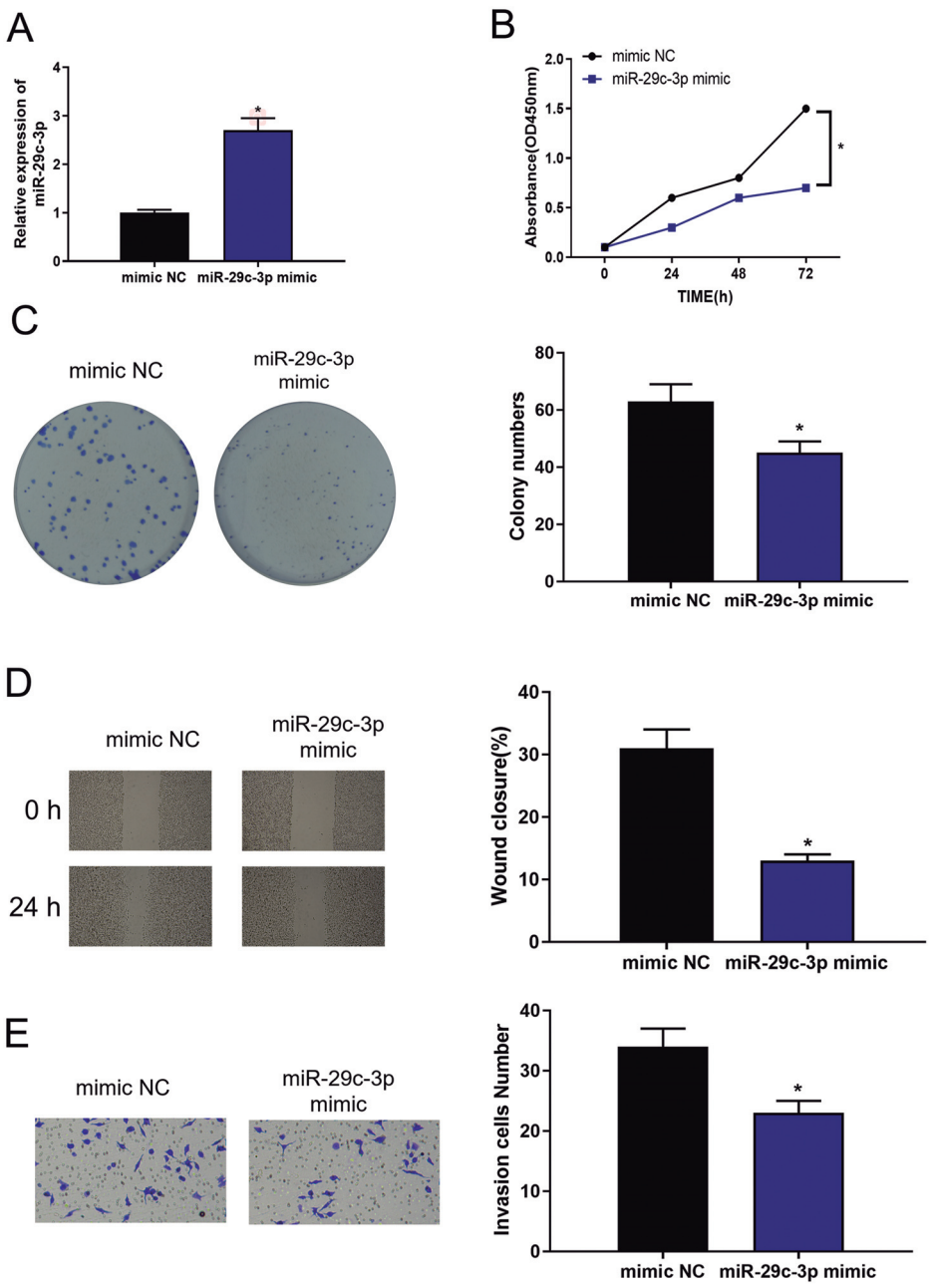

Fig. 2. MiR-29c-3p upregulation restrains GC cell functions. **A.** MiR-29c-3p expression in mimic NC or miR-29c-3p mimic groups. **B.** The viability of GC cells in miR-29c-3p mimic group was prominently downregulated. **C.** The proliferative ability of GC cells in miR-29c-3p mimic group was markedly downregulated. **D.** GC cell migratory ability after overexpressing miR-29c-3p. **E.** GC cell invasive ability after overexpression of miR-29c-3p. *p<0.05. D, x 40; E, x 100.

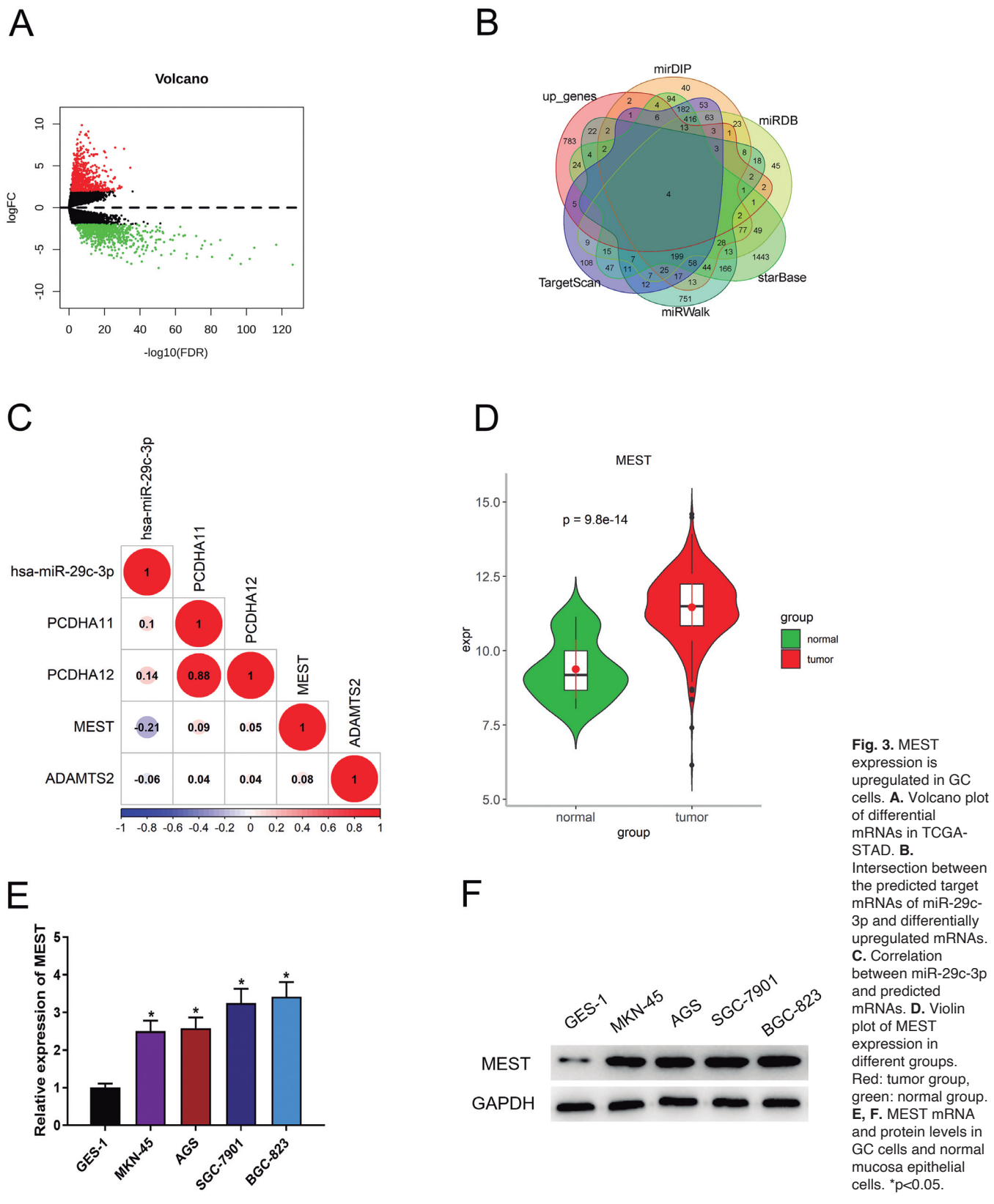

Fig. 3. MEST expression is upregulated in GC cells. **A.** Volcano plot of differential mRNAs in TCGA-STAD. **B.** Intersection between the predicted target mRNAs of miR-29c-3p and differentially upregulated mRNAs. **C.** Correlation between miR-29c-3p and predicted mRNAs. **D.** Violin plot of MEST expression in different groups. Red: tumor group, green: normal group. **E, F.** MEST mRNA and protein levels in GC cells and normal mucosa epithelial cells. *p<0.05.

mucosa epithelial cells (Fig. 3E-F). Thus, the results above suggested that MEST may be upregulated by miR-29c-3p in GC.

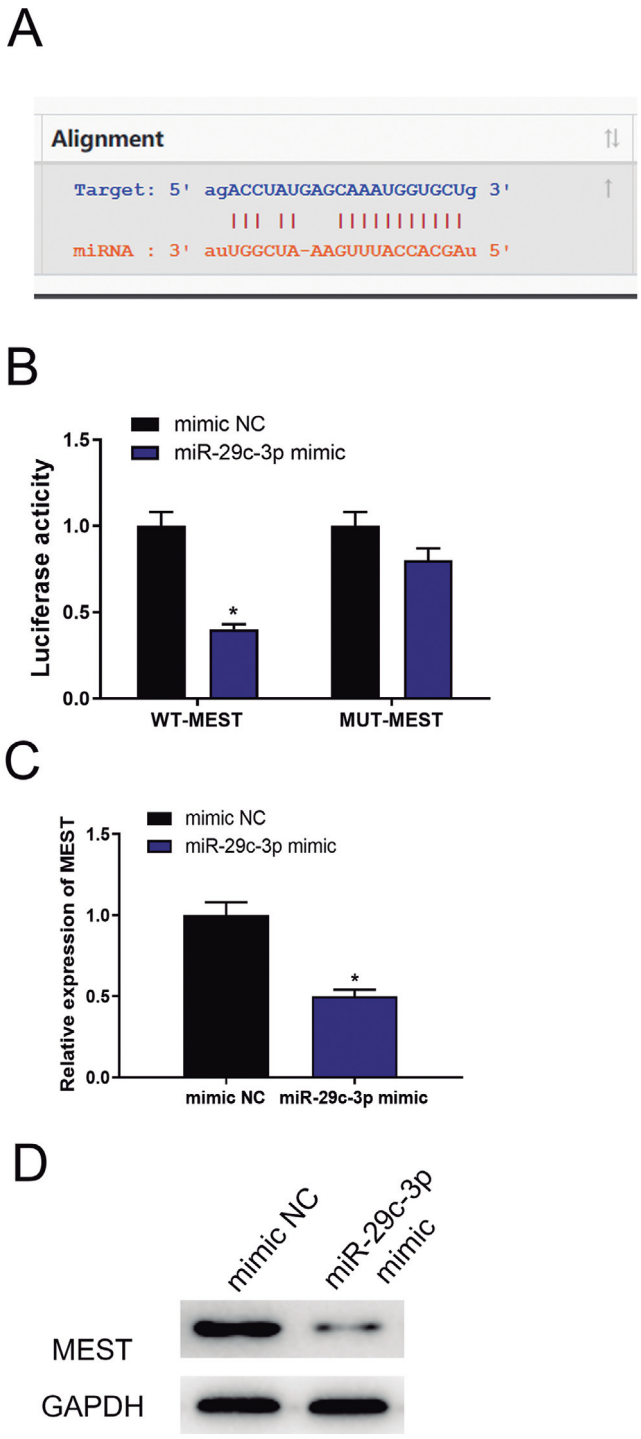

Fig. 4. MiR-29c-3p targets MEST. **A.** Binding sites of miR-29c-3p and MEST. **B.** Dual-luciferase assay testified that miR-29c-3p could bind with MEST. **C, D.** The effect of miR-29c-3p forced expression on MEST mRNA and protein levels. *p<0.05.

MEST is targeted and suppressed by miR-29c-3p

Additionally, bioinformatics method was applied to predict the binding sites of MEST 3'-UTR and miR-29c-3p (Fig. 4A). As detected by dual-luciferase method, miR-29c-3p mimic transfection markedly reduced luciferase activity of WT MEST 3'-UTR, while such transfection did not affect MUT MEST 3'-UTR (Fig. 4B). qRT-PCR and western blot detection discovered that MEST mRNA and protein expression was conspicuously lower in miR-29c-3p mimic group than in mimic NC group (Fig. 4C,D). The above results were consistent with bioinformatics analysis, indicating that MEST was targeted and repressed via miR-29c-3p.

MiR-29c-3p represses MEST expression to affect GC cell proliferation, migration and invasion

In the context, highly-expressed MEST in GC cells was negatively correlated with miR-29c-3p expression. In addition, miR-29c-3p upregulation restrained GC cell behaviors. To further verify their regulation, rescue assay was used. As detected by qRT-PCR and western blot, miR-29c-3p forced MEST level to reduce markedly (Fig. 5A,B). Cell proliferative assay suggested that MEST overexpression alone remarkably elevated cancer cell proliferative ability compared with control group. However, cancer cell proliferative ability was prominently more restrained in miR-29c-3p mimic+oe-MEST group than in mimic NC+oe-MEST group (Fig. 5C,D). Wound healing and Transwell assays indicated that compared with the NC group, the overexpression of MEST significantly strengthened the cell migratory and invasive abilities, while simultaneously overexpressed miR-29c-3p would reverse the promotion effects caused by MEST overexpression on GC cells (Fig. 5E,F). Taken together, MEST was able to simulate GC cell progression, and the promotion was counteracted by miR-29c-3p overexpression. We considered that miR-29c-3p modulated GC cell behaviors via repressing MEST expression.

Discussion

GC is a prevalent tumor with poor prognosis and high mortality (Xiao et al., 2011). Despite great progress in diagnosis and treatment, the therapeutic results of GC remain unsatisfactory(Xiao et al., 2011). Inhibiting tumor cell proliferation, migration and invasion can prevent tumor occurrence (Liu et al., 2019). miRNAs can bind to 3'-UTR of target mRNAs to directly degrade target mRNAs or repress target mRNA translation, thereby regulating biological processes of cells, such as migration, differentiation, apoptosis and transformation (Bayoumi et al., 2016). In this study, mature miRNA expression data in TCGA-STAD were firstly downloaded from TCGA database to determine significantly decreased miR-29c-3p expression in GC. Moreover, bioinformatics methods predicted that MEST may act as a downstream negative regulatory gene. We

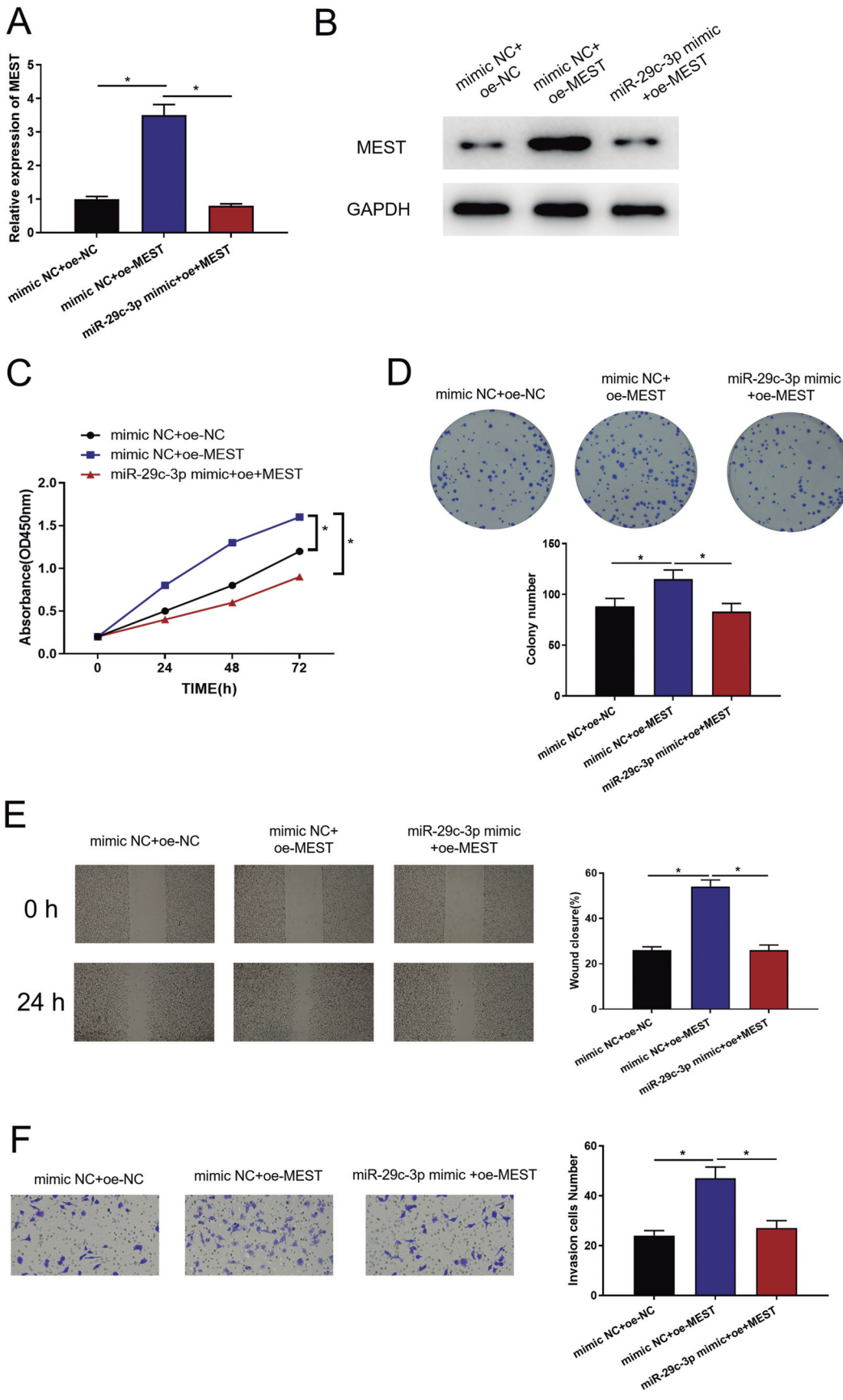

Fig. 5. MiR-29c-3p represses MEST to regulate GC cell functions. **A, B.** MEST mRNA and protein levels in transfection groups (mimic NC+oe-NC, mimic NC+oe-MEST, miR-29c-3p mimic+oe-MEST). **C.** Viability of GC cells in each group. **D.** Proliferative ability of GC cells in each group. **E.** Cell migratory ability in each group. **F.** Cell invasive ability in each group. *p<0.05. E, x 40; F, x 100.

also focused on researching the regulation between miR-29c-3p with MEST and their effect on GC cell functions, which may offer new ideas for future GC therapy.

Firstly, we noticed that miR-29c-3p expression in GC cells was suppressed, which was in agreement with a previous study (Han et al., 2019). MiR-29c-3p is associated with the occurrence of various cancers in many studies. For instance, miR-29c-3p level in HCC is downregulated, which is intimately relevant to poor prognosis of HCC patients (Wu et al., 2019). In ovarian cancer, miR-29c-3p can target and inhibit KIF4A expression, thus potentiating cancer cell proliferation and migration (Xu et al., 2020). MiR-29c-3p suppresses GC cell proliferation and migration in vitro and in vivo by regulating the expression of KIAA1199 (Wang et al., 2019). Here, miR-29c-3p was underexpressed in GC cell lines, and GC cell progression was inhibited as miR-29c-3p elevated. Hence, miR-29c-3p may repress GC cancer cell progression.

Thereafter, qRT-PCR and western blot assays found that MEST mRNA and protein levels were markedly upregulated in GC cells. It has been reported that MEST plays a promoter or inhibitor role in varying cancers. For example, high MEST expression induces EMT in fibroblast cell line in breast cancer (Kim et al., 2019). Furthermore, MEST was a direct target gene of ZFP57 and was significantly upregulated in breast cancer tissue (Chen et al., 2019), while ZFP57 constrains breast cancer cell proliferation via downregulating the Wnt/β-catenin signaling pathway mediated by MEST (Chen et al., 2019). MEST expression is relatively low in ovarian cancer cells (Ruan and Zhao, 2019). In this study, dual-luciferase assay testified the interaction between miR-29c-3p and MEST. Rescue assay was undertaken to further understand their regulation and the effect of MEST on GC cells. Rescue assay indicated that overexpression of miR-29c-3p significantly reversed the promotion effect of MEST on the proliferation, migration and invasion of GC cells. These results indicate that MEST was a downstream regulatory gene of miR-29c-3p and facilitated GC progression as a cancer promoter.

Altogether, we verified that miR-29c-3p downregulation was relevant to GC occurrence, and miR-29c-3p repressed MEST expression. This work unveiled that miR-29c-3p exerted tumor inhibitory effects on GC progression by modulating MEST, and a new insight into the clinical treatment of GC patients is provided.

Ethics approval and consent to participate. Not applicable.

Consent for publication. Not applicable.

Competing interests. No conflicts of interest.

Funding. Not applicable.

Data Availability. The data used to support the findings of this study are available from the corresponding author upon request.

Authors' contributions. HHL and QJJ both conceived and designed the analysis. JQL performed the experiments and collected the data. JDW performed the data analyses. HFW wrote the original manuscript. LL performed the analysis with constructive discussions.

References

Ajani J.A., Bentrem D.J., Besh S., D'Amico T.A., Das P., Denlinger C., Fakih M.G., Fuchs C.S., Gerdes H., Glasgow R.E., Hayman J.A., Hofstetter W.L., Ilson D.H., Keswani R.N., Kleinberg L.R., Korn W.M., Lockhart A.C., Meredith K., Mulcahy M.F., Orringer M.B., Posey J.A., Sasson A.R., Scott W.J., Strong V.E., Varghese T.K., Jr., Warren G., Washington M.K., Willett C., Wright C.D., McMillian N.R., Sundar H. and National Comprehensive Cancer N. (2013). Gastric cancer, version 2.2013: Featured updates to the NCCN guidelines. J. Natl. Compr. Canc. Netw. 11, 531-546.

Bayoumi A.S., Sayed A., Broskova Z., Teoh J.P., Wilson J., Su H., Tang Y.L. and Kim I.M. (2016). Crosstalk between long noncoding RNAs and micrornas in health and disease. Int. J. Mol. Sci. 17, 356.

Chen L., Wu X., Xie H., Yao N., Xia Y., Ma G., Qian M., Ge H., Cui Y., Huang Y., Wang S. and Zheng M. (2019). ZFP57 suppress proliferation of breast cancer cells through down-regulation of MEST-mediated Wnt/beta-catenin signalling pathway. Cell Death Dis. 10, 169.

Ferlay J., Shin H.R., Bray F., Forman D., Mathers C. and Parkin D.M. (2010). Estimates of worldwide burden of cancer in 2008: Globocan 2008. Int. J. Cancer 127, 2893-2917.

Han Y., Wu N., Jiang M., Chu Y., Wang Z., Liu H., Cao J., Liu H., Xu B. and Xie X. (2019). Long non-coding RNA myoslid functions as a competing endogenous RNA to regulate mcl-1 expression by sponging miR-29c-3p in gastric cancer. Cell Prolif. 52, e12678.

Kim M.S., Lee H.S., Kim Y.J., Lee D.Y., Kang S.G. and Jin W. (2019). MEST induces Twist-1-mediated EMT through STAT3 activation in breast cancers. Cell Death Differ. 26, 2594-2606.

Liu G.H., Liu Y.H., Yang Z., Zhu A.L. and Zhao C.L. (2016). MicroRNA-524-5p suppresses the growth and invasive abilities of gastric cancer cells. Oncol. Lett. 11, 1926-1932.

Liu H.M., Wu Q., Cao J.Q., Wang X., Song Y., Mei W.J. and Wang X.C. (2019). A phenanthroline derivative enhances radiosensitivity of hepatocellular carcinoma cells by inducing mitochondria-dependent apoptosis. Eur. J. Pharmacol. 843, 285-291.

McGuire A., Brown J.A. and Kerin M.J. (2015). Metastatic breast cancer: The potential of miRNA for diagnosis and treatment monitoring. Cancer Metastasis Rev. 34, 145-155.

Morita S., Horii T., Kimura M., Ochiya T., Tajima S. and Hatada I. (2013). MiR-29 represses the activities of DNA methyltransferases and DNA demethylases. Int. J. Mol. Sci. 14, 14647-14658.

Raitoharju E., Seppala I., Oksala N., Lyytikainen L.P., Raitakari O., Viikari J., Ala-Korpela M., Soininen P., Kangas A.J., Waldenberger M., Klopp N., Illig T., Leiviska J., Loo B.M., Hutri-Kahonen N., Kahonen M., Laaksonen R. and Lehtimaki T. (2014). Blood microRNA profile associates with the levels of serum lipids and metabolites associated with glucose metabolism and insulin resistance and pinpoints pathways underlying metabolic syndrome: The cardiovascular risk in young finns study. Mol. Cell Endocrinol. 391, 41-49.

Ruan Z. and Zhao D. (2019). Long intergenic noncoding RNA LINC00284 knockdown reduces angiogenesis in ovarian cancer cells *via* up-regulation of MEST through NF-κB1. FASEB J. 33, 12047-12059.

Wang L., Yu T., Li W., Li M., Zuo Q., Zou Q. and Xiao B. (2019). The miR-29c-KIAA1199 axis regulates gastric cancer migration by binding with WBP11 and PTP4A3. Oncogene 38, 3134-3150.

Wu H., Zhang W., Wu Z., Liu Y., Shi Y., Gong J., Shen W. and Liu C. (2019). MirR29c-3p regulates DNMT3B and LATS1 methylation to

inhibit tumor progression in hepatocellular carcinoma. Cell Death Dis. 10, 48.

Xiao X.Y., Hao M., Yang X.Y., Ba Q., Li M., Ni S.J., Wang L.S. and Du X. (2011). Licochalcone a inhibits growth of gastric cancer cells by arresting cell cycle progression and inducing apoptosis. Cancer Lett. 302, 69-75.

Xu H., Mao H.L., Zhao X.R., Li Y. and Liu P.S. (2020). MiR-29c-3p, a target miRNA of LINC01296, accelerates tumor malignancy: Therapeutic potential of a LINC01296/miR-29c-3p axis in ovarian cancer. J. Ovarian Res. 13, 31.

Zhang R., Wang G., Zhang P.F., Zhang J., Huang Y.X., Lu Y.M., Da W., Sun Q. and Zhu J.S. (2017a). Sanguinarine inhibits growth and invasion of gastric cancer cells via regulation of the DUSP4/ERK pathway. J. Cell Mol. Med. 21, 1117-1127.

Zhang S., Jin J., Tian X. and Wu L. (2017b). Hsa-mir-29c-3p regulates biological function of colorectal cancer by targeting SPARC. Oncotarget 8, 104508-104524.

Zhou W., Pal A.S., Hsu A.Y., Gurol T., Zhu X., Wirbisky-Hershberger S.E., Freeman J.L., Kasinski A.L. and Deng Q. (2018). MicroRNA-223 suppresses the canonical NF-κB pathway in basal keratinocytes to dampen neutrophilic inflammation. Cell Rep. 22, 1810-1823.

Accepted October 21, 2022